IOSR Journal of Applied Physics (IOSR-JAP)
e-ISSN: 2278-4861.Volume 8, Issue 2 Ver. I (Mar. - Apr. 2016), PP 114-119
www.iosrjournals.org

Optical Transition Probabilities of Er^{3+} doped TiO_2 Prepared via Sol-Gel

Hanaa M. Yaseen[1] Bassam G. Rasheed[2] And Sabah N. Mazhir[3]
[1,3] *College Of Sciences For Woman, Baghdad University, Baghdad, Iraq*
[2] *College Of Engineering, Al-Nahrin University, Baghdad, Iraq*

Abstract: *Spectroscopic properties of Er:TiO2 samples have been investigated at room temperature, the samples are prepared with different doping rate by using Sol Gel method. A Judd-Ofelt analysis is used to analysis the UV- Visible spectra (in range of 400-900nm) and calculate the three Judd-ofelt of parameters;* Ω_2, Ω_4 *and* Ω_6. *From the obtained parameters, the radiative transition probabilities A(J;J'), radiative lifetime* τ_{rad} *and fluorescence branching ratio* $\beta_{J\rightarrow J'}$ *were calculated. The optical properties of prepared doped samples are close to the known of Er:YAG optical property. Due to these suitable optical properties of doped sample, the* $Er:TiO_2$ *has the potential to be a laser material and serious may find its application in eye-safe near-infrared laser systems.*

Keywords: *Sol-Gel; Spectroscopy;* TiO_2*; laser active medium.*

1. Introduction

In recent years, great interest focus on preparing of optical material, several methods developed to synthesis rare earth ions doped with different host medium. Due low temperature and high homogeneity, the wet chemical process is one of favour method to prepare transparent monoliths containing rare earth ions as active ions [1-6]. The sol-gel process has been widely considered a suitable process to fabricate optical materials with various configurations, such as monoliths, coatings, fibbers and films for optical device applications. The formation of oxide particles in a liquid phase, leads to make the structure of sol-gel materials inherently porous. Using of acid and base catalysts makes the reaction process (hydrolysis and condensation) to become faster [7-10]. In the present study, we have performed the Judd–Ofelt theory to analyzes the Absorption spectra to calculate the spectroscopic properties of $Er^{3+}:TiO_2$, especially the transition probabilities A(J;J'), radiative lifetime τ_{rad} and branching ration $\beta_{J\rightarrow J'}$ of Er^{3+} ion.

II. Experimental

The doped and un-doped samples were synthesized by sol–gel method from Titanium (IV)- iso–propoxide (TTIP) (Aldrich 98%), hydrochloric acid HCl 34.5% from BDH, Ethanol (EtOH 99.9%) from GCC, and Erbium(III) nitrate pentahydrate (Aldrich). Deionized water was used for the hydrolysis of (TTIP) and preparation of pure and doped TiO_2 sol. The reaction process was conducted at room temperature. The amount of each chemical in this procedure was TEIP:H_2O:EtOH:HCl= 1:1:10:0.1 in molar ratio. All solution was prepared as follows: 1 mole of Titanium (IV)- iso–propoxide (TTIP) and ethanol (EtOH) were mixed and stirred for 10 min. At the stirring time, 0.1 M catalysts in water were added drop wise to the solution until water to TTIP molar ratio reach to around two. Erbium (III) nitrate pentahydrate is solve in ethanol and then used for mixing with TTIP. All solutions leaved to stir for about 2 hours further at room temperature before use.

Samples with covers left to aged for 24 hours in room temperature in order to complete the hydrolysis process and permit solvent evaporation through the drying process. The doping rates of samples with Er^{3+} is equal to 1.24%wt, 2.65%wt, 3.78% wt, 5.05%wt and 6.31%wt. Absorption spectra at room temperature were obtained with Shimdzu UV-VIS Spectrophotometer (in range of 400-900nm).

III. Results

Room temperature UV-VIS-NIR absorption spectra of the Er^{3+} doped sample are presented in Figure (1). The absorption spectrum is well resolved so that almost every peaks or stark components corresponding to different manifold of Er^{3+} are observed to measure the integrated absorption cross section for each peak or manifold. The so-called line strength, S_{meas}, can be found by **Eq. 1** [11]:

$$S_{meas}(J \rightarrow J) = \frac{3ch(2J+1)\ n}{8\pi^3 e^2 \overline{\lambda}\ \rho_o}\ \left[\frac{3}{n^2+2}\right]^2\ \Gamma---(1)$$

Where J and J' are the total angular momentum of the initial ground and final manifold, the value of J found from the $^{2S+1}L_J$ designation, ρ_o is the Er^{3+} ion concentration, n is the refractive indices of the host medium, $\overline{\lambda}$ is the mean wavelength of the specific absorption peak corresponds to the $J \rightarrow J'$ transition, while e, c and h have their usual meaning. Γ is the integrated absorption coefficient and given by [11]:

$$\Gamma = \int_{manifolds} \alpha(\lambda)d\lambda - - - (2)$$

Where $\alpha(\lambda)$ is the absorption coefficient as a function of wavelength λ. The S_{meas} , $\overline{\lambda}$ and integrated absorption coefficients are displayed in **Table (1)**.

Table (1): Value of Line Strength S_{meas} , Average wavelength $\overline{\lambda}$ and Absorption cross section Γ for each transitions of Er doped TiO$_2$ with doping rate equal to 1.24, 2.65% , 3.78%, 5.05% and 6.31%wt.

Transitions from $^4I_{15/2}$	1.24%wt		2.65%wt		3.78%		5.05%wt		6.31%wt	
	$\overline{\lambda}$ (nm)	Γ (nm cm^{-1})	$\overline{\lambda}$ (nm)	Γ (nm cm^{-1})	$\overline{\lambda}$ (nm)	Γ (nm cm^{-1})	$\overline{\lambda}$ (nm)	Γ (nm cm^{-1})	$\overline{\lambda}$ (nm)	Γ (nm cm^{-1})
$^4F_{7/2}$	498	.0925	498	.2228	498	.293	498	.5613	498	.316
$^2H_{11/2}$	523	.687	523	1.333	523	1.969	523	2.914	523	1.8989
$^4S_{3/2}$	555	.03515	555	.040	555	.0912	555	.113	555	.0804
$^4F_{9/2}$	653	.201	653	.4584	653	.713	653	1.15	653	.6963
$^4I_{9/2}$	802	.0777	802	.1323	802	.1317	802	.2394	802	.296

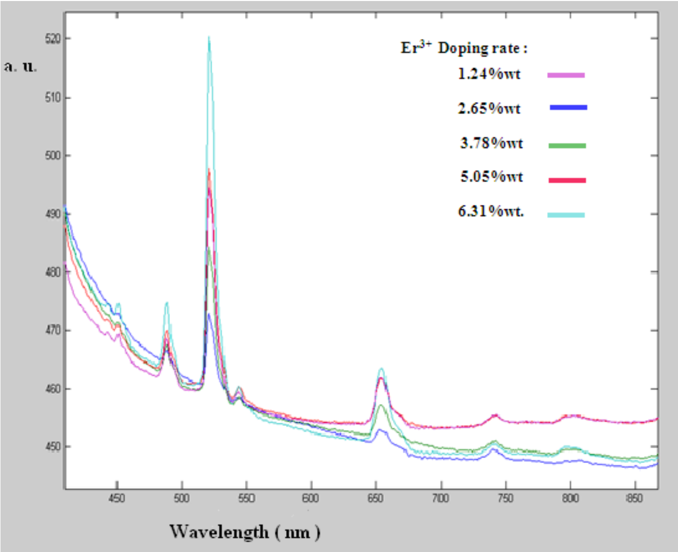

Figure 1: The Absorption spectra for Er:TiO$_2$ with different doping rate.

According to the Judd-Ofelt JO theory, the line strength between initial manifold J and terminal manifold J' may be written in the form [11]:

$$S_j^t = \sum_{i=1}^{3} M_{ij}\,\Omega_i \quad - - - -(3)$$

Where Ω_i is the Judd-Ofelt parameters which represents components of [1 x 3] matrix for Judd-Ofelt parameters (include to three parameters; Ω_2, Ω_4 and Ω_6). M_{ij} is doubly reduced matrix (or square matrix elements) and represented components of N x 3 matrix for square matrix elements $U^{(2)}$, $U^{(4)}$ and $U^{(6)}$. N represents the number of transitions to fit, which depends on the number of absorption manifolds actually measured. The square matrix element does not depend on host materials [12-14]. We have used the values of the $U^{(2)}$, $U^{(4)}$ and $U^{(6)}$ which calculated by Carnall *et al.* [15-17], **Table (2)** involve the value of $U^{(2)}$, $U^{(4)}$ and $U^{(6)}$ to Er^{3+} ions for transition from ground state manifold $^4I_{15/2}$ to some exited manifolds.

The parameters Ω_i determined the transition strength between any two energy levels in these active ions. These parameters could be found using the $\boldsymbol{S_{meas}}$ values (that obtained from equation (1)) into equation (3) in addition to the square matrix elements $U^{(2)}$, $U^{(4)}$ and $U^{(6)}$. The values of the three parameters; Ω_2, Ω_4 and Ω_6 can then be used to recalculate the transition line strengths of the absorption bands using Eq.3. The values of the measured absorption line strengths, S_{meas} , S_{calc} and the three JO parameters are tabulated in **Table (3)**. While **Table (4)** involve the Judd-Ofelt parameters Ω_i for Er:TiO_2 samples with different doping rate.

Table (2) Values of the square matrix elements $U^{(2)}$, $U^{(4)}$ and $U^{(6)}$

Transitions from $^4I_{15/2}$	$U^{(2)}$	$U^{(4)}$	$U^{(6)}$
$^4F_{7/2}$	0	0.1469	0.6266
$^2H_{11/2}$	0.7125	0.4125	0.0925
$^4S_{3/2}$	0	0	0.2211
$^4F_{9/2}$	0	0.5354	0.4618
$^4I_{9/2}$	0	0.1733	0.0099

Table (3): Value of S_{meas} , and S_{calc} for each transitions of Er:TiO_2

Transitions from $^4I_{15/2}$	**1.24%wt**		**2.65%wt**		**3.78%**		**5.05%wt**		**6.31%wt**	
	S_m $*10^{-20}$ (cm^{-1})	**S_{CAL} *10-20 (cm^{-1})**	**S_m $*10^{-20}$ (cm^{-1})**	**S_{CAL} *10-20 (cm^{-1})**	**S_m $*10^{-20}$ (cm^{-1})**	**S_{CAL} *10-20 (cm^{-1})**	**S_m $*10^{-20}$ (cm^{-1})**	**S_{CAL} *10-20 (cm^{-1})**	**S_m $*10^{-20}$ (cm^{-1})**	**S_{CAL} *10-20 (cm^{-1})**
$^4F_{7/2}$	**0.09448**	0.096	**0.1066**	0.104	**0.0983**	0.142	**0.14117**	0.142	**0.063**	0.061
$^2H_{11/2}$	**0.6873**	0.687	**0.6247**	0.624	**0.6475**	0.717	**0.71797**	0.717	**0.374**	0.374
$^4S_{3/2}$	**0.0341**	0.021	**0.0181**	0.023	**0.0290**	0.033	**0.02701**	0.033	**0.015**	0.012
$^4F_{9/2}$	**0.1753**	0.178	**0.1873**	0.187	**0.2044**	0.242	**0.24703**	0.242	**0.119**	0.123
$^4I_{9/2}$	**0.0576**	0.044	**0.0459**	0.046	**0.0321**	0.057	**0.04371**	0.057	**0.043**	0.032

Table (4): Judd–Ofelt parameters and spectroscopic quality factors of Er:TiO_2 with different doping rate.

Er3+ Doping Rate	**Ω_2**	**Ω_4**	**Ω_6**	**quality factor Ω_4 /Ω_6**
1.24%wt	**0.8063**	**0.2522**	**0.0951**	**2.6519**
2.65%wt	**0.712**	**0.259**	**0.1056**	**2.4606**
3.78%	**0.7342**	**0.2781**	**0.1037**	**2.6813**
5.05%wt	**0.8015**	**0.3221**	**0.1512**	**2.1296**
6.31%wt	**0.412**	**0.182**	**0.085**	**2.141**

The phenomenological J-O parameters can now be subsequently utilized to determine emission line strengths S_{calc} corresponding to the transitions from the upper multiplet manifolds states $^4I_{13/2}$, $^4I_{11/2}$, $^4I_{9/2}$, $^4F_{9/2}$, $^4S_{3/2}$, $^2H_{11/2}$, $^4F_{7/2}$ and $^2G_{9/2}$ to their corresponding lower-lying manifold states Er^{3+} in TiO_2, the S_{calc} are calculated by using Eq. 3. The values S_{calc} are used to find the radiative transition probabilities *A(J;J')* for each excited upper manifolds states to the $^4I_{J'}$, $^4S_{J'}$ and $^4F_{J'}$ manifold for Er^{3+} , the *A(J;J')* for Er^{3+} in the initial *J* manifold. *J'* is the final manifold is given in Eq. (4) [11]:

$$A(J;J) = \frac{64\,\pi^4}{3h\,(2J+1)\lambda^3}\left[\frac{n(n^2+2)^2}{9}\right]S_{calc} \quad \text{---(4)}$$

The radiative lifetime τ_{rad} is given by [11]:

$$\tau_{rad} = 1 \,/\, \sum A(J;J) \;............... \;(5)$$

where the sum is over all final lower-lying states J. The radiative transition probabilities *A(J;J')* rates for the Er^{3+} transitions in **TiO_2** hosts are determined by using Eq. (4); these values are given in Table (5) and (6). The values of the *A(J;J')* are added to obtain the total radiative rates for the $^4I_{13/2}$, $^4I_{11/2}$, $^4I_{9/2}$, $^4F_{9/2}$, $^4S_{3/2}$, $^2H_{11/2}$, $^4F_{7/2}$, and $^2G_{9/2}$ manifold states. The radiative lifetimes of these levels are determined by Eq. (5). These values are given in **Table (5) and (6)**. The transitions from the individual excited state to the lower-lying manifolds should have the same measured lifetime because they all originate from the same excited state. Therefore, while the predicting radiative lifetime of an individual upper level, according to the Judd–Ofelt analysis, one should add the all value of *A(J;J')* for the corresponding transitions from that level to all lower levels and then invert the sum according to the Eq. (5) [18].

The fluorescence branching ratio $\beta_{J\rightarrow J'}$ is a critical parameter to the laser designer, because it characterizes the possibility of attaining stimulated emission from any specific transition. The fluorescence branching ratios can be determined from the *A(J;J')* rates by:

$$\beta_{J\rightarrow J'} = \frac{A(J;J')}{\sum_{J'} A(J;J')}$$

The calculated results of *A(J;J')* are listed in **Table (5) and (6)**. The results show that Er:tiO2 samples with doping rate 1.24%wt , 2.65%wt , 3.78%wt, 5.05%wt and 6.31%wt have radiative transition probabilities *A(J;J')* of $^4I_{13/2}\rightarrow{}^4I_{15/2}$ equal to 101 sec^{-1}, 95 sec^{-1}, 98 sec^{-1} ,113sec^{-1} and 57.2 sec^{-1} respectfully. These result are comparable to those of Er:YAG (121 sec^{-1})[18], Er:YSGG (126 sec^{-1})[18] , Er:YSGG (130 sec^{-1})[18], Er$_x$Y$_{1-x}$Al$_3$(BO$_3$)$_4$ (233sec^{-1}) [19], and Er:La$_2$CaB$_{10}$O$_{19}$ (262 sec^{-1}) [20]. Due to the high concentrations of Er^{3+} activators with good optical properties; the Er:TiO$_2$ sample has the potential to be a laser material.

Table (5) The transition probabilities A(J;J') and branching ration $\beta_{J\rightarrow J'}$ of Er^{3+}:TiO$_2$ with doping rate 1.24%wt, 2.65%wt and 3.78%wt.

Transition		1.24%wt			2.65%wt			3.78%		
from	To	A$_{rad}$ (sec^{-1})	$\beta_{J\rightarrow J'}$	τ $_{rad}$ (m sec)	A$_{rad}$ (sec^{-1})	$\beta_{J\rightarrow J'}$	τ $_{rad}$ (m sec)	A$_{rad}$ (sec^{-1})	$\beta_{J\rightarrow J'}$	τ $_{rad}$ (m sec)
$^4I_{13/2}\rightarrow$	$^4I_{15/2}$	101.76	1	9.826	95.59	1	10.461	98.81	1	10.12
$^4I_{11/2}\rightarrow$	$4I_{15/2}$	112.86	0.881	7.812	115.8	0.878	7.588	115.55	0.877	7.593
	$4I_{13/2}$	15.13	0.118		15.97	0.121		16.13	0.122	
$^4I_{9/2}\rightarrow$	$4I_{15/2}$	140.59	0.84	5.981	145.04	0.831	5.732	155.03	0.842	5.433
	$4I_{13/2}$	25.89	0.154		28.66	0.164		28.23	0.153	
	$4I_{11/2}$	0.69	0.004		0.73	0.004		0.75	0.004	
$^4F_{9/2}\rightarrow$	$4I_{15/2}$	1150.7	0.908	0.789	1208.26	0.911	0.754	1265.76	0.912	0.721
	$4I_{13/2}$	67.24	0.053		68.48	0.051		72	0.051	
	$4I_{11/2}$	43.75	0.034		45.37	0.034		45.22	0.032	
	$4I_{9/2}$	4.31	0.003		3.84	0.002		3.95	0.002	
$^4S_{3/2}\rightarrow$	$4I_{15/2}$	238.56	0.656	2.753	264.9	0.657	2.483	260.24	0.656	2.523
	$4I_{13/2}$	98.86	0.272		109.78	0.272		107.84	0.272	
	$4I_{11/2}$	8.63	0.023		9.49	0.023		9.43	0.023	
	$4I_{9/2}$	17.03	0.046		18.31	0.045		18.67	0.047	
	$4F_{9/2}$	0.12	0		0.13	0		0.13	0	
$^2H_{9/2}\rightarrow$	$4I_{15/2}$	714.67	0.316	0.442	780.39	0.339	0.434	781.61	0.333	0.427
	$4I_{13/2}$	1151.34	0.509		1140.59	0.495		1167.9	0.498	
	$4I_{11/2}$	325.39	0.144		315.07	0.137		326.02	0.139	
	$4I_{9/2}$	42.63	0.018		38.7	0.016		40.04	0.017	
	$4F_{9/2}$	24.89	0.011		24.88	0.01		25.68	0.01	
$^4F_{7/2}\rightarrow$	$4I_{15/2}$	1517.92	0.691	0.455	1639.06	0.7	0.427	1662.88	0.691	0.415
	$4I_{13/2}$	426.74	0.194		439.7	0.187		470.68	0.195	
	$4I_{11/2}$	170.55	0.077		177.35	0.075		186.75	0.077	
	$4I_{9/2}$	75.23	0.034		78.95	0.033		80.15	0.033	
	$4F_{9/2}$	5.28	0.002		5.09	0.002		5.34	0.002	
	$4S_{3/2}$	0.68	0		0.64	0		0.65	0	
$^2H_{11/2}\rightarrow$	$4I_{15/2}$	8759.26	0.958	0.109	7960.99	0.957	0.12	8251.46	0.956	0.115
	$4I_{13/2}$	143.88	0.015		139.5	0.016		145.17	0.016	
	$4I_{11/2}$	88	0.009		85.57	0.01		89.82	0.01	
	$4I_{9/2}$	111.51	0.012		103.28	0.012		105.99	0.012	
	$4F_{9/2}$	33.08	0.003		29.33	0.003		30.25	0.003	
	$4S_{3/2}$	0.03	0		0.04	0		0.04	0	

Table (6) The transition probabilities A(J;J') and branching ration $\beta_{J\to J'}$ of Er^{3+}:TiO_2 with doping rate 5.05%wt and 6.31%wt.

Transition		5.05%wt			6.31%		
from	To	A_{rad} (sec^{-1})	$\beta_{J\to J'}$	τ rad (m sec)	A_{rad} (sec^{-1})	$\beta_{J\to J'}$	τ rad (m sec)
$4I_{13/2}$ →	$^4I_{15/2}$	113.8	1	8.787	57.76	1	17.312
$4I_{11/2}$ →	$4I_{15/2}$	154.45	0.877	5.683	69.28	0.876	12.651
	$4I_{13/2}$	21.5	0.122		9.76	0.123	
$4I_{9/2}$→	$4I_{15/2}$	180.33	0.811	4.5	93.47	0.84	8.989
	$4I_{13/2}$	40.87	0.183		17.29	0.155	
	$4I_{11/2}$	0.97	0.004		0.45	0.004	
$4F_{9/2}$→	$4I_{15/2}$	1558.49	0.911	0.584	766.14	0.913	1.192
	$4I_{13/2}$	85.87	0.05		43.21	0.051	
	$4I_{11/2}$	61.08	0.035		27.2	0.032	
	$4I_{9/2}$	4.35	0.002		2.26	0.002	
$4S_{3/2}$→	$4I_{15/2}$	379.49	0.659	1.738	159.54	0.656	4.117
	$4I_{13/2}$	157.26	0.273		66.11	0.272	
	$4I_{11/2}$	13.36	0.023		5.76	0.023	
	$4I_{9/2}$	24.75	0.043		11.36	0.046	
	$4F_{9/2}$	0.19	0		0.08	0	
$2H_{9/2}$→	$4I_{15/2}$	1085.19	0.363	0.334	477.31	0.34	0.713
	$4I_{13/2}$	1439.19	0.482		693.9	0.494	
	$4I_{11/2}$	385.21	0.129		192.47	0.137	
	$4I_{9/2}$	44.51	0.014		23.14	0.016	
	$4F_{9/2}$	31.34	0.01		15.31	0.01	
$4F_{7/2}$→	$4I_{15/2}$	2232.75	0.716	0.32	1012.87	0.693	0.684
	$4I_{13/2}$	545.16	0.174		283.71	0.194	
	$4I_{11/2}$	225.72	0.072		112.75	0.077	
	$4I_{9/2}$	105.23	0.033		48.43	0.033	
	$4F_{9/2}$	6.12	0.001		3.15	0.002	
	$4S_{3/2}$	0.79	0		0.38	0	
$^2H_{11/2}$→	$4I_{15/2}$	9149.17	0.955	0.104	4771.6	0.956	0.2
	$4I_{13/2}$	169.65	0.017		85.78	0.017	
	$4I_{11/2}$	103.28	0.01		53.15	0.01	
	$4I_{9/2}$	122.36	0.012		61.62	0.012	
	$4F_{9/2}$	33.07	0.003		17.33	0.003	
	$4S_{3/2}$	0.05	0		0.02	0	

IV. Conclusion

The transparent and unbroken sample of Er^{3+} doped NanoTitnia successfully prepared by wet chemical synthesis method. Through Appling of Judd-Ofelt theory to evaluate the optical transition probabilities of Er^{3+} ions in TiO_2, it found that optical properties of prepared doped samples are close similar to the known of Er:YAG optical properties. This suggests that it could be use Sol-Gel technique to prepare of Er:TiO_2 as solid state Laser active medium, Er:TiO_2 are serious may find its application in eye-safe near-infrared laser systems.

V. Acknowledgements

Authors would like to thank Physics Department, College of sciences for woman, Baghdad University for all assistance in preparation and correspondences to this study.

References

[1]. Mohammed Alwan Hamzah, Anwar M. Ezzat, Majida A. Ameen, Hanaa M. Yaseen and Mnaa I. Khalif, " Preparations of Nd:TiO2 as Laser active medium by Sol-Gel method" , International Journal of Application or Innovation in Engineering & Management (IJAIEM), Volume 3, Issue 5, May 2014.

[2]. X. Chen and W. Luo, "Optical Spectroscopy of Rare Earth Ion-Doped TiO2 Anophosphors," Journal of Nanoscience and Nanotechnology, Vol. 10, No. 3, 2010, pp. 1482- 1494

[3]. Hanaa M. Yaseen, Bassam G. Rasheed, Sabah N. Mazhir, "Judd–Ofelt Analysis of Spectroscopic Properties of Er+3:Tio2 Prepared Via Sol-Gel", IOSR Journal of Research & Method in Education, Volume 6, Issue 2 Ver. III (2016), PP 30-33.

[4]. Mohammed Alwan Hamzah, Majida A. Ameen, Fuad M. Mutar and Hanaa M. Yaseen, "Optical properties of Nd3+:SiO2 Prepared via Sol-Gel", International Journal of Application or Innovation in Engineering & Management (IJAIEM), Volume 3, Issue 5, May 2014.

[5]. Mohammed A. Hamza, F. Saiof, A. Al-ithawi, M. Ameen and H. Yaseen, "Prepared of Nd: TiO_2 Nano Particles Powder as IR Filter via Sol-Gel," Advances in Materials Physics and Chemistry, Vol. 3 No. 2, 2013, pp. 174-177. doi: 10.4236/ampc.2013.32024.

[6]. Mohammed A. Hamza, Asmaa Sh. Khalil, Hanna M. Yaseen, " Synthesis of Yb3+ Doped TiO2 Nano Particles Powder as IR Filter via Sol-Gel", Advances in Materials Physics and Chemistry, 2013, 3, 214-216.

[7]. C. Jeffrey Brinker , George W. Scherer "The PHYSICS AND CHEMISTRY of Sol-Gel processing", SOL-GEL SCIENCE Academic press,(1990).

[8]. J. Livage, M. Henry and C. Sanchez, "Sol-Gel Chemistry of Transition Metal Oxides," Progress in Solid State Chemistry, Vol. 18, No. 4, 1988, pp. 259-342. doi:10.1016/0079-6786(88)90005-2

[9]. Majida A. A., Asmaa J. K. and Anwar A. B., "Annealing Effect on the phase Transformation in Sol-Gel Derived Titania Nanostructures", Baghdad Science Journal 8 (2), 503-508, 2011.

[10]. Mohammed. A. Hamza, Majeda A. Ameen and Hanaa M. Yaseen, "Judd–Ofelt analysis of Spectroscopic properties of Nd+3:SiO2 Prepared via Sol-Gel", Eng. & Tech.Journal, Vol.33, Part (B), No.5, 2015.

[11]. B. Walsh, "Judd-Ofelt Theory: Principles and Practices," in Advances in Spectroscopy For Lasers and Sensing, pp. 403–433, Springer, NewYork, NY,USA, 2006.

[12]. B. R. Judd, "Optical absorption intensities of rare-earth ions,"Physical Review, vol. 127, no. 3, pp. 750–761, 1962.G. S.

[13]. Ofelt, "Intensities of crystal spectra of rare-earth ions," Journal of Chemical Physics, vol. 37, no. 3, p. 511, 1962.

[14]. H. P. Nicholas Verlinden, (2008), " The Excited State Absorption Cross Section of Neodymium-doped Silica Glass Fiber in the 1200-1500 nm Wavelength Range," Phd thesis WORCESTER POLYTECHNIC INSTITUTE

[15]. Carnall W. T. and Crosswhite H. M., (1977), "Energy level structure and transition probabilities in the spectra of the trivalent lanthanides in LaF3", Technical report, Argonne National Laboratory.

[16]. Carnall W. T., Goodman G. L., Rajnak K. and Rana R. S., (1988) "A systematic analysis of the spectra of the lanthanides doped into single crystal LaF3", Technical Report ANL-88-8, Argonne National Laboratory.

[17]. Carnall W. T., Fields P. R., and K. Rajnak, (1968), "Electronic energy levels in the trivalent lanthanide aquo ions. I. Pr^{3+}, Nd^{3+}, Pm^{3+}, Sm^{3+}, Dy^{3+}, Ho^{3+}, Er^{3+} and Tm^{3+}", J. Chem. Phys., Vol.49, pp4424–4442.

[18]. Dhiraj K. Sardar, William M. Bradley, and John J. Perez, "Judd–Ofelt analysis of the Er^{3+} $^4F_{11}$ absorption intensities in Er^{3+} doped garnets", JOURNAL OF APPLIED PHYSICS VOLUME 93, NUMBER 5, MARCH 2003.

[19]. M. G. Liu, B. S. Lu, H. F. Pan, and Q. Song, "ErxY1−xAl3(BO3)4 crystal growth and its spectral properties," Acta Optical Sinica, vol. 8, pp. 1079–1084, 1988.

[20]. R.Guo,Y.Wu, P. Fu, and F. Jing, "Optical transition probabilities of Er3+ ions in La2CaB10O19 crystal," Chemical Physics Letters, vol. 416, no. 1–3, pp. 133–136, 2005.